CHAPTER 8

Effects of a novel polyphenol-rich plant extract on body composition, inflammation, insulin sensitivity and glucose homeostasis in obese mice

Hendrik J.P. van der Zande, Joost M. Lambooij, Vivien Chavanelle, Anna Zawistowska-Deniziak, Yolanda Otero, Frank Otto, Louise Lantier, Owen P. McGuinness, Florian Le Joubioux, Martin Giera, Thierry Maugard, Sébastien L. Peltier, Pascal Sirvent and Bruno Guigas

International Journal of Obesity. 45:2016–2027 (2021)
PMID: 34079069
doi: 10.1038/s41366-021-00870-x

Abstract

Background/Objectives: The worldwide prevalence of obesity, metabolic syndrome and type 2 diabetes (T2D) is reaching epidemic proportions that urge the development of new management strategies. Totum-63 is a novel, plant-based polyphenol-rich active principle that has been shown to reduce body weight, fasting glycemia, glucose intolerance and fatty liver index in obese subjects with prediabetes. Here, we investigated the effects and underlying mechanism(s) of Totum-63 on metabolic homeostasis in insulin-resistant obese mice.

Methods: Male C57BL6/J mice were fed a high-fat diet for 12 weeks followed by supplementation with Totum-63 for 4 weeks. The effects on whole-body energy and metabolic homeostasis, as well as on tissue-specific inflammation and insulin sensitivity were assessed using a variety of immunometabolic phenotyping tools.

Results: Totum-63 decreased body weight and fat mass in obese mice, without affecting lean mass, food intake and locomotor activity, and increased fecal energy excretion and whole-body fatty acid oxidation. Totum-63 reduced fasting plasma glucose, insulin and leptin levels, and improved whole-body insulin sensitivity and peripheral glucose uptake. The expression of insulin receptor β and the insulin-induced phosphorylation of Akt/PKB were increased in liver, skeletal muscle, white adipose tissue (WAT) and brown adipose tissue (BAT). Hepatic steatosis was also decreased by Totum-63 and associated with a lower expression of genes involved in fatty acid uptake, *de novo* lipogenesis, inflammation and fibrosis. Furthermore, a significant reduction in proinflammatory macrophages was also observed in epididymal WAT. Finally, a potent decrease in BAT mass associated with enhanced tissue expression of thermogenic genes was found, suggesting BAT activation by Totum-63.

Conclusions: Our results show that Totum-63 reduces inflammation and improves insulin sensitivity and glucose homeostasis in obese mice through pleiotropic effects on various metabolic organs. Altogether, plant-derived Totum-63 might constitute a promising novel nutritional supplement for alleviating metabolic dysfunctions in obese people with or without T2D.

Introduction

The dramatic worldwide rise in obesity, insulin resistance (IR), metabolic associated fatty liver disease (MAFLD), and type 2 diabetes (T2D) poses a serious global threat to public health. The most recent data from the World Health Organization indicate that more than a third of the world's adult population is overweight (1) and 465 million suffer from T2D (2), with an associated yearly health care cost estimated to exceed 760 billion dollars (3). T2D is a complex and multifactorial disease that develops as a result of synergistic dysfunctions of metabolic pathways in interconnected organs, such as the intestine, pancreas, liver, skeletal muscle, adipose tissues and the brain (4, 5). During the last decade it also became clear that the immune system plays a central role in disease progression, with the obesity-associated chronic low-grade inflammation, or metaflammation (6), being one of the major contributors to tissue-specific IR and impaired glucose/lipid homeostasis (7-10). While some treatments with various drug classes are available, the multiplicity of the pathophysiological mechanisms involved in T2D development makes pharmacological interventions targeting a single pathway generally insufficient. In this context, therapeutic strategies simultaneously targeting several dysfunctional mechanisms in different organs may constitute the most efficient option for tackling these complex and multifactorial metabolic disorders.

The concepts of functional foods and nutraceuticals have recently emerged and refer to a wide range of bioactive compounds contained in food and natural products with potentially relevant benefits on human health (11, 12). As such, several plants used in traditional medicines or as dietary supplements contain antioxidants, fibers and phytochemicals, like polyphenols and alkaloids, that have been shown to exert anti-obesogenic and antidiabetic properties through concomitant modulation of diverse cellular pathways and metabolic processes (13-17). Although still mechanistically unclear, these bioactive compounds can exert pleiotropic actions on multiple tissues, leading to beneficial metabolic effects such as appetite reduction, modulation of intestinal nutrient absorption and metabolism, enhanced thermogenesis, improvement of tissue-specific insulin sensitivity and/or changes in both gut microbiota and local/systemic inflammation (13).

Totum-63 is a novel, polyphenol-rich plant-based active principle composed of a mixture of five plant extracts that has been designed to act in combination to target the risk factors associated with developing T2D. Totum-63 has recently been shown to reduce body weight, fasting glycemia, glucose intolerance and fatty liver index in a clinical study conducted in obese subjects with prediabetes (18). In the present study, we aimed to investigate the effects and underlying mechanism(s) of Totum-63 on metabolic homeostasis in high-fat diet (HFD)-induced obese mice, a model of established T2D.

Results

Totum-63 decreases body weight and fat mass, and reduces food efficiency in obese mice

To study the effects of Totum-63 on metabolic homeostasis in insulin resistant obese mice, C57BL/6 male mice were first fed a high-fat diet (HFD) for 12 weeks, followed by supplementation with or without Totum-63 (2.7% w/w) for 4 additional weeks (Figure 1A). Totum-63 induced a rapid decrease in body weight in HFD-fed obese mice, which was already significant after 6 days of supplementation (Figure 1B). At the end of the experimental period, the body weight remained significantly lower in the Totum-63-supplemented mice (Figure 1C), an effect exclusively due to a reduction in body fat mass (Figure 1D) and associated with lower liver (Figure 1E) and BAT (Figure 1F) masses while both WAT and heart weights were not affected (Figure 1G-H). Food intake, assessed by regular weighing of food pellets, was found to be transiently reduced during the first days of Totum-63 supplementation, without affecting the average food intake throughout the entire study (Figure 1I-J). Next, using individual metabolic cages, we confirmed that Totum-63 neither altered food intake after the first day of supplementation (Supplementary Figure 1A) nor spontaneous locomotor activity (Supplementary Figure 1B) and total energy expenditure (Supplementary Figure 1C) in HFD-fed obese mice. However, indirect calorimetry revealed that Totum-63 significantly decreased the respiratory exchange ratio (RER; Supplementary Figure 1D), indicating that whole-body fatty acid oxidation was increased while carbohydrate oxidation was concomitantly decreased (Supplementary Figure 1E-F). Of note, although the fecal energy content was not affected by Totum-63 supplementation in HFD-fed mice (Figure 1L), the feces production rate was increased (Figure 1K) and, as such, the daily amount of excreted energy (Figure 1M). Since the daily ingested energy was not different (Figure 1N), the calculated apparent energy assimilation efficiency (AEAE) was therefore reduced by Totum-63 in obese mice (Figure 1O), suggesting that an alteration of nutrient absorption in the digestive tract may partly contribute to the reduction in body weight. Of note, no significant changes in the expression of the main fatty acid (FA) and carbohydrate (CHO) intestinal transporters were observed, at least in the ileum, while the expression of the biliary cholesterol transporters *Abcg5* and *Abcg8* were significantly upregulated by Totum-63 (Figure 1P). Congruent with this, ileal expression of the bile acid (BA)-regulated gene *Fgf15* (19) was also upregulated by Totum-63, whereas the expression of other gut-derived hormones was unchanged (Supplementary Figure 2A). Moreover, Totum-63 supplementation restored the gene expression of tight junction proteins involved in HFD-induced intestinal permeability (Figure 1Q), but did not affect the expression of inflammatory markers in the ileum (Supplementary Figure 2B).

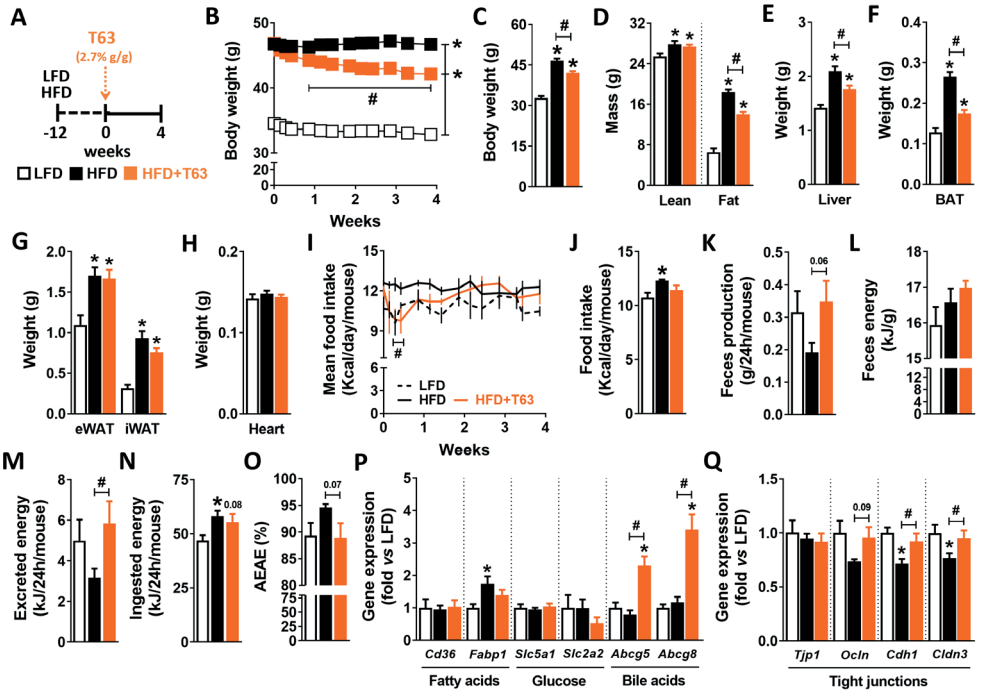

Figure 1. Totum-63 decreases body weight, fat mass and energy assimilation efficiency in HFD-fed mice. (**A**) C57BL6/J mice were fed either a low-fat diet (LFD, open squares/bars) or high-fat diet (HFD) for a period of 12 weeks after which the HFD was supplemented with Totum-63 (T63, 2.7% g/g; orange squares/bars) or not (control; black squares/bars) for an additional 4 weeks. (**B**) Body weight was monitored throughout the supplementation period. (**C-D**) At week 4, body weight and body composition were determined. (**E-H**) After sacrifice, the weights of the liver (*E*), BAT (*F*), eWAT, iWAT (*G*) and heart (*H*) were measured. (**I-J**) Mean food intake per mouse was monitored throughout the supplementation period. (**K**) The feces production was assessed during 24 hours. (**L**) The fecal energy content was determined by bomb calorimetry. (**M-O**) The excreted (*M*) and ingested (*N*) energy, and the apparent energy assimilation efficiency (AEAE, *O*) were calculated. (**P-Q**) The expression of key genes involved in nutrient and bile transport (*P*) and epithelial tight junctions (*Q*), was measured in the ileum section of the intestine by RT-qPCR. Results are expressed as mean ± SEM. * P ≤ 0.05 *vs* LFD, # P ≤ 0.05 *vs* HFD (n=10-12 mice per group from 2 independent experiments; feces: n=3-5 cages per group; qPCR: n=5-6 mice per group).

Totum-63 improves glucose homeostasis and insulin sensitivity in obese mice

We next investigated the effects of Totum-63 on whole-body metabolic homeostasis in HFD-fed obese mice. As expected, HFD feeding increased fasting plasma glucose, insulin and leptin levels (Figure 2A-C), HOMA-IR (HOmeostatis Model Assessment of Insulin Resistance; Figure 2D), as well as blood HbA1c levels (Figure 2E) when compared to LFD-fed mice. Furthermore, HFD impaired whole-body insulin sensitivity (Figure 2F) and glucose

homeostasis (Figure 2G-H), as assessed by intraperitoneal insulin and glucose tolerance tests, respectively. Totum-63 supplementation in HFD-fed mice restored glucose, insulin and HOMA-IR, as well as blood HbA1c to the LFD-fed mice levels (Figure 2A-B, D-E) while circulating leptin concentrations were significantly reduced (Figure 2C). Congruent with HOMA-IR data, Totum-63 improved whole-body insulin sensitivity and glucose homeostasis in obese mice, as respectively assessed by insulin and glucose tolerance tests (Figure 2F-G), without affecting glucose-induced insulin levels (Figure 2H). Importantly, all these beneficial effects were still observed in a subset of body weight-paired control and supplemented obese mice (Supplementary Fig 3), indicating that the improvement of metabolic homeostasis by Totum-63 is not only secondary to reduced body weight. Of note, the effect on glucose, insulin and HOMA-IR was already observed after 2 weeks of Totum-63 supplementation whereas fasting total cholesterol (TC) and triglycerides (TG) were not affected (Supplementary Figure 4). Moreover, the HFD-induced increase in total blood leukocyte counts and circulating levels of monocytes and B cells was still present after Totum-63 supplementation, while other myeloid (neutrophils, eosinophils) and lymphoid (NK, T) cells were not affected whatever the conditions (Supplementary Figure 5).

In order to decipher the respective contribution of the main metabolic organs to the improvement of systemic insulin sensitivity by Totum-63 in obese mice, we performed a hyperinsulinemic-euglycemic clamp. Blood glucose levels were maintained at euglycemia in all mice during the clamp whereas insulinemia was found to be significantly lower at steady state in HFD-fed mice treated with Totum-63 (Figure 3A-B). As expected, the glucose infusion rate (GIR) was markedly reduced in HFD-fed obese mice when compared to lean mice, but the extent of this detrimental effect was significantly lower in Totum-63-treated mice (Figure 3C). Although the endogenous glucose production rate (EndoRa) was unchanged (Figure 3D), the glucose disappearance rate (Rd) was found to be significantly improved by Totum-63 in HFD-fed obese mice (Figure 3E-F). Administration of 2-^{14}C-DG during the clamp was used to determine insulin-stimulated glucose uptake (Rg) in various tissues. As shown in Figure 3G-H, Totum-63 increased insulin-induced skeletal muscle Rg in HFD-fed mice, regardless of muscle type, while a borderline significant trend for an increase was also observed in heart, eWAT and BAT. In line with this, the insulin receptor β expression (IRβ) and insulin-induced phosphorylation of protein kinase B (PKB) were found to be increased by Totum-63 in all tissues (Figure 3I-L), indicating improvement in both hepatic and peripheral insulin sensitivity in HFD-fed mice.

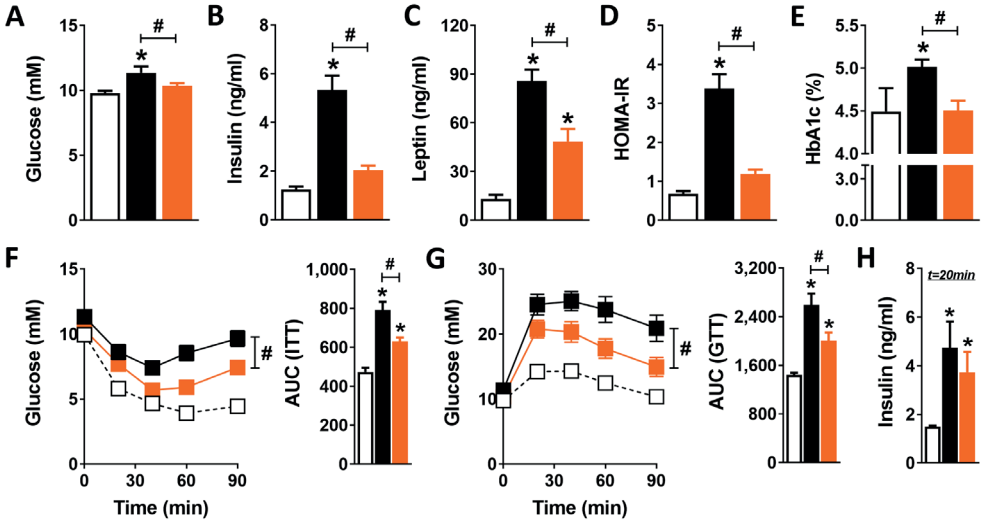

Figure 2. Totum-63 improves whole body metabolic homeostasis in obese mice. LFD- and HFD-fed C57BL6/J mice were treated as described in the legend of Figure 1. (**A-E**) Fasting blood glucose (*A*) and plasma insulin (*B*) levels were measured at week 4 of supplementation and used to calculate the HOMA-IR (*D*). Fasting plasma leptin (*C*) and blood HbA1c (*E*) levels were also determined at the same time point. (**F**) At week 3, whole-body insulin sensitivity was determined by an intraperitoneal (i.p.) insulin tolerance test (ITT) in 4-h fasted mice. Blood glucose levels were measured at the indicated timepoints after i.p. insulin injection and the AUC was calculated. (**G-H**) An i.p. glucose tolerance test (GTT) was performed at week 4 of supplementation in 6-h fasted mice. Blood glucose levels were measured at the indicated timepoints and the AUC was calculated (*G*). Plasma insulin levels during GTT were determined 20 min after glucose injection (*H*). Results are expressed as mean ± SEM. * P ≤ 0.05 *vs* LFD, # P ≤ 0.05 *vs* HFD (n=10-12 mice per group from 2 independent experiments).

Totum-63 reduces hepatic steatosis, inflammation and fibrosis in obese mice

Totum-63 supplementation almost completely reverted HFD-induced hepatic steatosis in obese mice, as assessed by H&E staining (Figure 4A-B) and liver total TG content (Figure 4C). Using quantitative lipidomics, we confirmed that Totum-63 significantly reduced the liver content of all TG species (Supplementary Figure 6). Furthermore, except for phosphatidylcholine levels that were found to be increased, the hepatic lipid composition of obese mice supplemented with Totum-63 resembled LFD-fed lean mice more than HFD-fed mice (Supplementary Figure 6A-C). This effect was associated with decreased gene expression of the major hepatic lipid transporters *Cd36* and *Fabp1*, and the lipogenic enzymes *Acaca*, *Fas* and *Scd1* when compared to HFD-fed control mice, whereas genes involved in FA oxidation were not affected (Figure 4D). Of note, Totum-63 also lowered the expression of *Fbp1*, one of the key gluconeogenic enzyme involved in hepatic glucose production (Figure 4E).

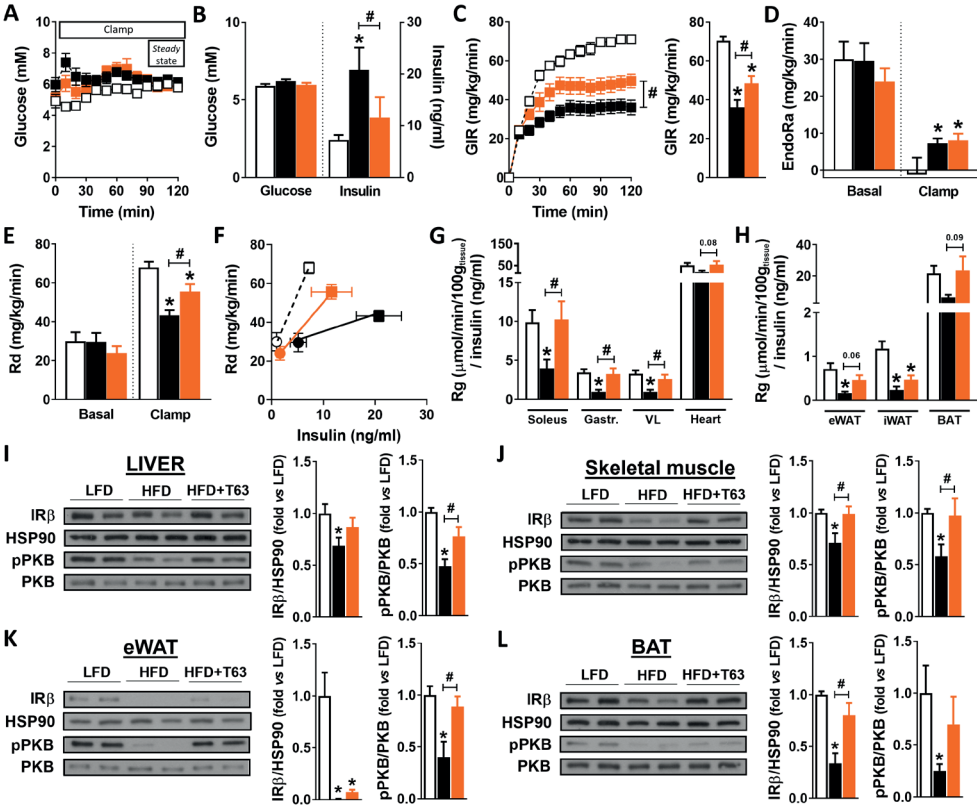

Figure 3. Totum-63 improves systemic and tissue-specific insulin sensitivity in obese mice. LFD- and HFD-fed C57BL6/J mice were treated as described in the legend of Figure 1. (**A**) A hyperinsulinemic-euglycemic clamp was performed in 5 h–fasted conscious mice. Blood glucose was monitored throughout the clamp at 10 min intervals by sampling from the arterial catheter. (**B**) Blood glucose and serum insulin levels were determined at steady-state (90-120 min). (**C**) The glucose infused rate (GIR) required to maintain euglycemia is shown. (**D-E**) The endogenous glucose production (EndoRa, *D*) and glucose disappearance rate (Rd, *E*) were determined using continuous infusion of ^{3}H-glucose. (**F**) The changes in Rd from basal to clamp state were plotted against the corresponding serum insulin levels. (**G-H**) The tissue-specific glucose uptake (Rg) was determined in soleus, gastrocnemius, vastus lateralis (VL), heart, eWAT, iWAT and BAT by administration of nonmetabolizable 2-[^{14}C]-deoxy-glucose and the data corrected for differences in serum insulin levels at steady state. (**I-L**) Tissue-specific insulin signaling was assessed in liver (*I*), quadriceps skeletal muscle (*J*), eWAT (*K*), and BAT (*L*) 15 min after an acute i.p. insulin injection. The protein expression of IRn PKB, and HSP90, and the phosphorylation (p) state of Ser473-PKB were determined by Western blot and quantified by densitometric analysis. The IRβ/HSP90 and pPKB/PKB ratios were calculated and expressed as fold change relative to LFD-fed mice. Results are expressed as mean ± SEM. * P ≤ 0.05 *vs* LFD, # P ≤ 0.05 *vs* HFD (clamp: n=6-8 mice per group; WB: n=5-10 mice per group from 2 independent experiments).

Activation of Kupffer cells (KCs), the tissue-resident macrophages, together with increased recruitment of monocyte-derived macrophages play a key role in obesity-induced hepatic inflammation and progression towards NASH and liver fibrosis (8). Using flow cytometry (see Supplementary Figure 7A for gating strategy), we showed that despite a trend for an increase, Totum-63 supplementation neither significantly affected total hepatic KCs content (Figure 4F) nor the HFD-induced increase in both $CD11c^+$ KCs (Figure 4G-H) and newly recruited monocytes (Figure 4I) in obese mice. This was also confirmed by the absence of differences in the hepatic gene expression of the pan monocyte/macrophage marker *Cd68* and KC marker *Clec4f* (Figure 4J). However, the expression of the proinflammatory chemokine/cytokine *Ccl2*, *Il1b* and *Tnf* were found to be significantly reduced by Totum-63 (Figure 4J), suggesting a reduction in HFD-induced KC activation. Furthermore, although the expression of the hepatic stellate cell marker *Hhipf* was not altered, those of early fibrotic markers *Acta2* and *Col1a1* were significantly reduced by Totum-63 in HFD-fed obese mice (Figure 4K).

Totum-63 reduces inflammation in white adipose tissues and promotes thermogenesis in brown adipose tissue from obese mice

Morphometric analysis of eWAT and iWAT using H&E staining revealed that Totum-63 supplementation in obese mice did not change mean adipocyte diameter and adipocyte size distribution (Figure 5A-B, F-G), a result in line with the absence of differences observed in tissue weights at sacrifice (Figure 1G). Using flow cytometry (see Supplementary Figure 7B for gating strategy), we showed that Totum-63 did not affect adipose tissue monocyte and total macrophage (ATM) contents (Figure 5C-D) but significantly lowered the percentage of obesity-associated $CD11c^+$ ATMs in eWAT (Figure 5E). In iWAT, a beneficial effect of Totum-63 on tissue inflammation was still observed, with a decrease in the number of immune cells per adipocyte observed by H&E staining (Figure 5H) and a reduction in the expression of proinflammatory gene markers (Figure 5I). Of note, the gene expression of thermogenic markers was not changed in iWAT from HFD-fed obese mice, indicating that Totum-63 did not promote WAT beiging (Figure 5I). By contrast to WAT, a significant reduction in both large adipocytes and adipocyte mean diameter was observed in BAT from obese mice supplemented with Totum-63 (Figure 6A-B). This result was in line with the potent decrease in organ weight observed at sacrifice and associated with an upregulation of most of the thermogenic genes (Figure 6C) and an increase in UCP1 protein expression (Figure 6D), suggesting BAT activation in obese mice supplemented with Totum-63. A decrease in the expression of HFD-induced proinflammatory genes was also evidenced in BAT (Figure 6E), highlighting again the beneficial impact of Totum-63 on metabolic tissue inflammation in obese mice.

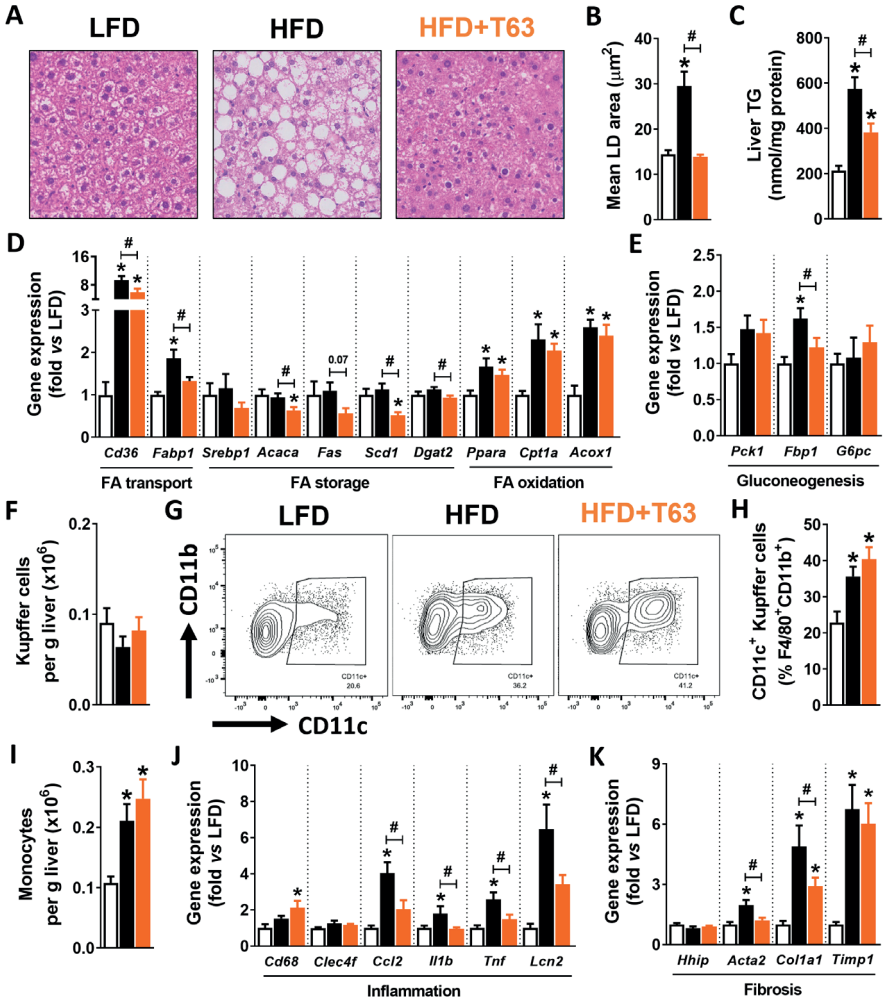

Figure 4. Totum-63 reduces hepatic steatosis, inflammation and fibrosis in obese mice. LFD- and HFD-fed C57BL6/J mice were treated as described in the legend of Figure 1. (**A-C**) Hepatic lipid droplet (LD) area by H&E staining (*A-B*) and liver triglyceride (TG) content (*C*) were determined to assess hepatic steatosis. (**D-E**) The hepatic expression of key genes involved in lipid metabolism (*D*) and gluconeogenesis (*E*) were measured by RT-qPCR. (**F-I**) The liver content of Kupffer cells (*F*) and monocytes (*I*) and the percentage of proinflammatory CD11c⁺ Kupffer cells (*G-H*) were determined by flow cytometry. (**J-K**) The hepatic expression of key genes involved in inflammation (*J*) and fibrosis (*K*) was measured by RT-qPCR. Results are expressed as mean ± SEM. * $P \leq 0.05$ *vs* LFD, # $P \leq 0.05$ *vs* HFD (hepatic steatosis: n=5-6 mice per group; flow cytometry: n=4-6 mice per group; qPCR: n=7-11 mice per group from 2 independent experiments).

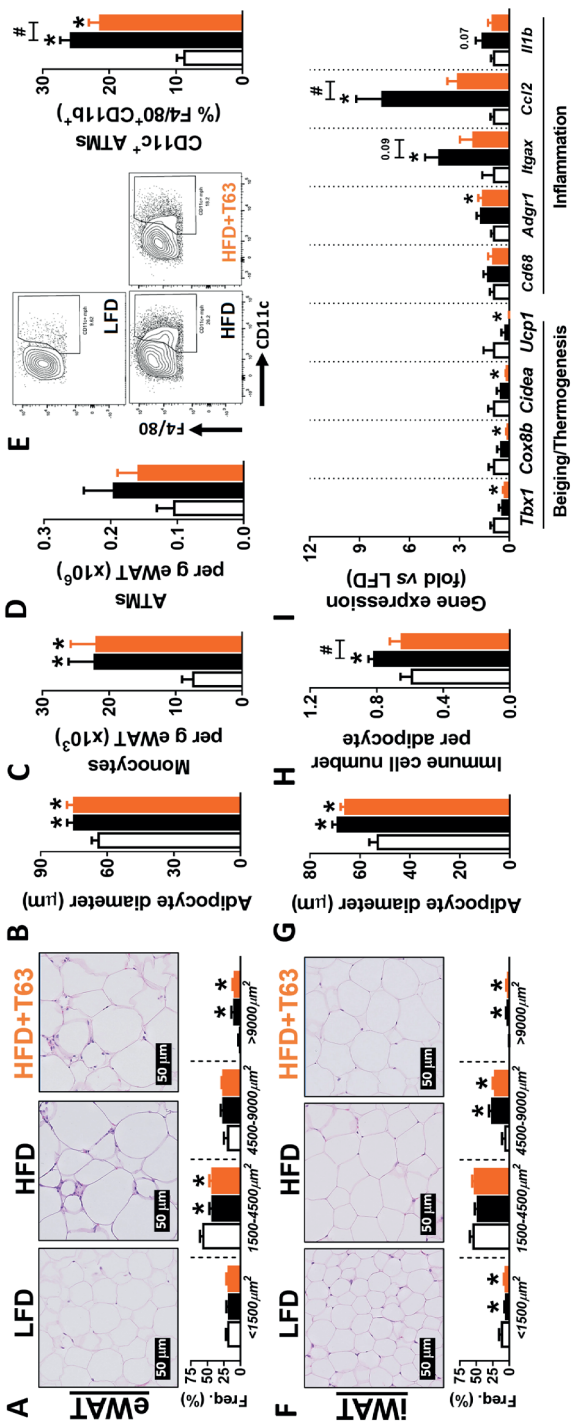

Figure 5. Totum-63 reduces inflammation in white adipose tissues from obese mice. LFD- and HFD-fed C57BL6/J mice were treated as described in the legend of Figure 1. (**A-G**) Adipocyte mean diameter and size distribution were determined by H&E staining in epididymal (eWAT, *A-B*) and inguinal (iWAT, *F-G*) adipose tissues. The number of eWAT monocytes (*C*) and adipose tissue macrophages (ATMs, *D*), and the percentage of obesity-associated CD11c$^+$ ATMs (*E*) were determined by flow cytometry. (**H-I**) The number of immune cell per adipocyte (*H*) and the expression of key genes involved in WAT beiging/thermogenesis and inflammation (*I*) were determined in iWAT by H&E staining and RT-qPCR, respectively. Results are expressed as mean ± SEM. * $P \leq 0.05$ *vs* LFD, # $P \leq 0.05$ *vs* HFD (adipocyte size/distribution: n=4-6 mice per group; flow cytometry: n=5-9 mice per group from 2 independent experiments; qPCR: n=5-6 mice per group).

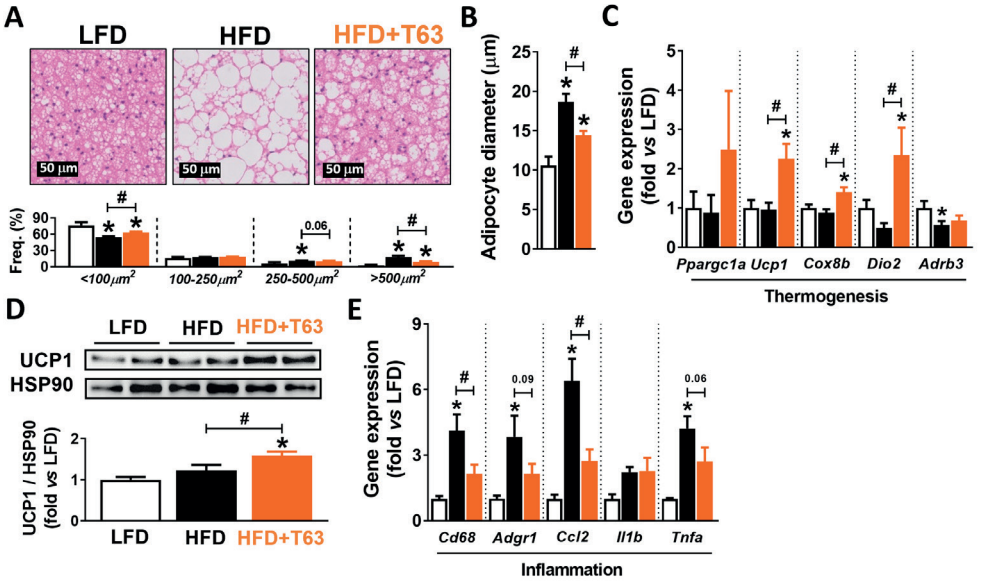

Figure 6. Totum-63 promotes thermogenic program and reduces inflammation in brown adipose tissue from obese mice. LFD- and HFD-fed C57BL6/J mice were treated as described in the legend of Figure 1. (**A-B**) Adipocyte mean diameter and size distribution were determined by H&E staining of subclavicular brown adipose tissue (BAT). (**C-E**) The expression of key genes involved in thermogenesis (*C*) and inflammation (*E*) was measured by RT-qPCR. The expression of UCP1 was assessed by Western Blot, and expressed relative to HSP90 (*D*). Results are expressed as mean ± SEM. * P ≤ 0.05 *vs* LFD, # P ≤ 0.05 *vs* HFD (adipocyte size/distribution: n=4-6 mice per group; qPCR: n=9-11 mice per group; WB: n=4 mice per group).

Discussion

The obesity and T2D epidemics urge new effective management strategies. The main objectives of the present study were to investigate the effects of Totum-63, a new polyphenol-rich plant-based nutritional supplement, on metabolic homeostasis in a mouse model of diet-induced obesity and T2D, and to decipher its underlying mechanism(s) of action. Here, we show that Totum-63 supplementation lowered body fat mass, reduced metaflammation, and improved both whole-body insulin sensitivity and glucose homeostasis in obese, insulin-resistant mice. These beneficial effects on obesity-associated low-grade inflammation and metabolic homeostasis were associated with either partial or almost complete restoration of various metabolic dysfunctions induced by HFD in different organs, suggesting a pleiotropic mode-of-action of Totum-63 owing to its chemical composition rich in various bioactive compounds.

We report that chronic consumption of Totum-63 through dietary supplementation significantly reduced body weight and fat mass in obese mice, a feature that was sustained

for at least 4 weeks while only associated with a transient reduction of food intake during the first days of supplementation, probably due to the bitterness of some flavonoids and saponins components of Totum-63. Whole-body EE was also not affected by Totum-63 throughout the study, a feature confirmed by ANCOVA analysis (data not shown), indicating that increased energy dissipation did not likely contribute in a significant and measurable extent to the reduction of body weight. By contrast, the daily feces production was increased and the AEAE was therefore significantly reduced, suggesting altered nutrient absorption and/or metabolism in the gastrointestinal tract. Interestingly, some bioactive compounds present in Totum-63, notably several polyphenols, have been previously reported to inhibit various digestive enzymes that may ultimately lead to a reduction in both carbohydrate and lipid absorption during the gastrointestinal transit (20-22). Among them, anthocyanins, chlorogenic acid, oleuropein and some luteolin derivatives have been shown to reduce both pancreatic α-amylase and lipase activities and inhibit intestinal α-glucosidase (20-22). Altogether, one can speculate that inhibition of digestive enzymes by various specific component(s) of Totum-63 may have contributed to the higher energy excretion in the feces observed in supplemented obese mice.

Since absorption of CHO and FA mostly takes place in the small intestine (23), we also measured ileal expression of some of the players involved in nutrient uptake and trafficking into enterocytes, but did not find any significant changes in response to Totum-63 supplementation. However, we cannot exclude that different intestinal segments could be affected and/or that alterations of other intestinal lumen-related processes might contribute to lower nutrient absorption, for instance through a decrease in passive diffusion of dietary TG-derived free FA (FFA) secondary to changes in gut permeability. In this context, it is worth mentioning that preliminary lipidomic analyses performed on pooled feces samples may support this hypothesis, as mean levels of various FFA species measured in Totum-63-supplemented mice were increased when compared to HFD-fed control mice (Supplementary Figure 8). In line with this, we also showed that Totum-63 can restore the HFD-induced downregulation of genes encoding tight junction proteins involved in obesity-associated intestinal permeability, dysbiosis and metaflammation (24). Once again, some Totum-63 components, including fibers and polyphenols, could directly and indirectly affect this interface, notably through modulation of local production of microbiota-derived metabolites that can act as signaling molecules and/or exert direct effects on the epithelial barrier (24). Altogether, further experiments are definitely required to explore the impact of Totum-63 on the gastrointestinal tract more in depth, not only focusing on nutrient absorption in various intestinal sections but also on microbiome composition and diversity, local immune responses and enterocyte-specific metabolic functions, which all can contribute to its beneficial effects.

The other important outcome of this study was the demonstration that Totum-63 can improve insulin sensitivity and glucose tolerance, an effect that is not entirely due to the observed reduction in body weight. Indeed, body weight-matching of control and supplemented obese mice showed that Totum-63 still exerted some intrinsic beneficial effects on metabolic homeostasis. Remarkably, we showed that Totum-63 supplementation in HFD-fed obese mice could restore insulin sensitivity and glucose uptake in various peripheral organs, notably in skeletal muscle, the tissue that contributes the most to the insulin-mediated glucose clearance from the circulation. Mechanistically, the obesity-associated metaflammation, which results from changes in the composition and activation states of various innate and adaptive immune cells in metabolic organs, has been suggested to underlie part of tissue-specific alterations of insulin signaling, notably in WAT and the liver (8-10). Interestingly, we found a mild but significant reduction in the $CD11c^+$ ATMs, a proinflammatory macrophage subset that is believed to mediate part of the detrimental effect on tissue insulin sensitivity (9, 25). In the liver, although $CD11c^+$ KC content was not affected, the decrease in gene expression of KC-derived cytokines such as *Ccl2* (MCP-1) and *Tnfa* suggests a reduction in HFD-induced KC proinflammatory activation by Totum-63. In line with this, Totum-63 also improved tissue-specific insulin sensitivity and induced a potent reduction in hepatic TG accumulation. This beneficial effect on liver steatosis was associated with a significant downregulation of genes involved in FA transport and *de novo* lipogenesis, while those involved in FA oxidation were unchanged. Taken together, this suggests that the reduction in ectopic lipid deposition in the liver may result from a decrease in both hepatic FA transport and TG biosynthesis, although we cannot exclude that it could also partly be the consequence of reduced lipid availability secondary to improved insulin-mediated inhibition of lipolysis in WAT and/or increased FA oxidation in BAT. Interestingly, we also found a decrease in BAT mass associated with an increased tissue expression of thermogenic genes, including *Ucp1*, in Totum-63-supplemented obese mice, suggesting BAT activation. However, we do not find a significant increase in EE, suggesting that the quantitative contribution of this effect to whole-body energy homeostasis is rather mild. Here again, some compounds present in Totum-63, notably chlorogenic acid and oleuropein, have been reported to promote BAT activation (26), at least partly through activation of the sympathetic nervous system (27). Alternatively, we show that Totum-63 increased ileal expression of BA-regulated genes, a feature that may suggest a higher BA bioavailability. In addition to their role in lipid absorption, BAs are increasingly recognized as signaling molecules that, among others, promote BAT activation and energy expenditure (28). Whether Totum-63 can affect liver and intestinal BA metabolism and whether this can contribute to some of its metabolic effects, notably through BA receptor-mediated BAT

activation, would require further studies. Of note, despite decreased hepatic expression of some early fibrotic gene markers by Totum-63, the HFD used in the framework of this study does not induce detectable levels of liver fibrosis, as assessed by Sirius red staining (data not shown). As such, further studies with appropriate NASH mouse models and/or pro-fibrotic diet regimens are also required to assess the impact of Totum-63 on fibrosis regression.

In conclusion, our current study shows that Totum-63, a new polyphenol-rich plant-based nutritional supplement, reduces body fat mass, hepatic steatosis, inflammation and insulin resistance in obese mice, likely through pleiotropic effects on various metabolic organs, including skeletal muscle, intestine, liver, and WAT/BATs. It is important to mention that in addition to the absence of an effect on locomotor activity, we have also not observed any abnormal behavioral/physiological parameters throughout the study that would have suggested some harmful effects. Furthermore, the impact of a 6-month supplementation with Totum-63 has also recently been evaluated in the framework of a phase 2a clinical trial in subjects with prediabetes (NCT02868177) and no detrimental side effects have been reported [18]. Altogether, although additional mechanistic and long-term studies are required, plant-derived Totum-63 appears to be a promising novel nutritional supplement for alleviating metabolic dysfunctions in obese people with or without T2D.

Materials and Methods

Totum-63

Totum-63 is a patented blend of 5 plant extracts designed to act in combination to target the risk factors of developing T2D. The mixture contains extracts from olive leaf (*Olea europaea*), bilberry (*Vaccinium myrtillus*), artichoke (*Cynara scolymus*), chrysanthellum (*Chrysanthellum indicum* subsp*. afroamericanum B.L. Turner*) and black pepper (*Piper nigrum*). Its chemical characterization is shown in Supplementary Table 1.

Animals and diet

All experiments were performed in accordance with the Guide for the Care and Use of Laboratory Animals of the Institute for Laboratory Animal Research and have received approval from the local Ethical Review Boards (Leiden University Medical Center, Leiden, The Netherlands; C2E2A, Clermont-Ferrand, France; Vanderbilt Animal Care and Use Committee, Nashville, USA). 10-week-old C57BL/6JOlaHsd male mice were purchased from Envigo (Horst, The Netherlands) and housed in a temperature-controlled room with a 12-hour light-dark cycle and *ad libitum* access to food and tap water. Mice were fed a low-fat diet (LFD, 10% energy derived from fat, D12450H, Research Diets, USA) or high fat diet (HFD, 45% energy derived

from fat, D12451, Research Diets, USA) for 12 weeks after which HFD was supplemented with or without Totum-63 (2.7% w/w, Valbiotis SA, Perigny, France) for an additional 4 weeks. A pilot study was performed *a priori* to select the most appropriate dosage of Totum-63 for reducing T2D risk factors in obese mice (data not shown). The experimental groups were randomized after removal of HFD low responders (~5%; body weight gain <6 g), according to total body weight, lean and fat mass, and fasting plasma glucose. An *a priori* power calculation was done. The experimenters were not blinded to the diet supplementation on the test days, however, most of the subsequent analyses were performed in blinded conditions.

Body composition and indirect calorimetry

Body weight was frequently measured during the 4 weeks of supplementation using a conventional weighing scale. Food intake was also frequently assessed by weighing food pellets in every cage. Body composition was measured at week 4 by MRI in conscious unrestrained mice using an EchoMRI (Echo Medical Systems). At sacrifice, visceral white adipose tissue (epididymal; eWAT), subcutaneous white adipose tissue (inguinal; iWAT), supraclavicular brown adipose tissue (BAT), heart and liver were weighed and collected for further processing. For indirect calorimetric measurements, 12-week HFD-fed mice were transferred to individual metabolic cages (8-channel multiplex system, Promethion, Sable Systems, USA) with free access to food and water, and followed for 4 weeks after the start of supplementation as previously reported (29) and described in the Appendix.

Insulin- and glucose tolerance tests

Whole-body insulin tolerance (ipITT) and glucose tolerance (ipGTT) tests were performed at week 3 and 4 of Totum-63 supplementation, respectively, as previously reported (29, 30) and described in the Appendix.

Hyperinsulinemic-euglycemic clamp

Hyperinsulinemic-euglycemic (HI-EU) clamp was performed at week 4 of supplementation. One week before HI-EU clamps, carotid artery and jugular vein catheters were surgically placed for sampling and infusions. Mice were fasted for 5h and then clamped unrestrained and in conscious state, as previously reported (31) and described in the Appendix.

Plasma analysis

Blood samples were collected from the tail vein of 4h-fasted mice using paraoxon-coated glass capillaries. Plasma total cholesterol (TC, Instruchemie #10015), triglycerides (TG,

Instruchemie #2913), insulin (Chrystal Chem #90080) and leptin (Chrystal Chem #90030), and whole blood HbA1c (Chrystal Chem #80310) were determined using commercially available kits per manufacturer's instructions. The homeostatic model assessment of insulin resistance (HOMA-IR) adjusted for mice (32) was calculated as followed ([glucose (mg/dl)*0.055]*[insulin (ng/ml)*172.1])/3875.

Feces analyses

Feces were carefully collected from 24h cage bedding during week 4 and weighed. Fecal energy density was determined by bomb calorimetry (IKA C200, Germany). The apparent energy assimilation efficiency (AEAE) was calculated as (fecal energy density x averaged daily feces production / averaged daily energy intake over the collection period).

Hepatic lipid composition

Liver lipids were measured as previously reported (33, 34) and described in the Appendix.

Histological analysis

Pieces of eWAT, iWAT, BAT and liver (~30 mg) were fixed in 4% formaldehyde (Sigma-Aldrich), paraffin-embedded, sectioned at 4 μm and stained with Hematoxylin and Eosin (H&E) (30). Six fields at 20x magnification were used for the analysis of adipocyte diameter and hepatic steatosis.

Isolation of leukocytes from blood, adipose tissue and liver for flow cytometry

At sacrifice, blood was collected retro-orbitally in heparin-coated tubes for leukocytes isolation as described in the Appendix and previously reported (29, 30). After a 1-minute post sacrifice transcardial perfusion with PBS, eWAT and liver samples were collected and digested for isolation of either stromal vascular fraction or leukocytes, respectively, as previously reported (29, 30) and described in the Appendix.

Flow cytometry

Analysis of blood, WAT and liver myeloid/lymphocyte subsets were done as previously reported (29, 30) and described in the Appendix.

RNA-isolation and RT-qPCR

RNA was extracted from snap-frozen liver, eWAT, iWAT, BAT or intestine samples using TriPure RNA Isolation reagent (Roche Diagnostics). Total RNA (1-2 μg) was reverse

transcribed using the M-MLV Reverse Transcriptase kit (ThermoFisher). Real-time qPCR runs were performed on a CFX96 Real-time C1000 thermal cycler (Biorad) using the GoTaq qPCR Master Mix kit (Promega). Gene expression was normalized using housekeeping gene *RplP0* and expressed as fold change compared to LFD-fed mice. Primer sequences can be found in Supplementary Table 2.

Western blot analysis

Snap-frozen liver, skeletal muscle (quadriceps), eWAT and BAT samples (~50 mg) collected 15 min after an acute i.p. insulin injection (1U/kg lean body mass) were lysed in ice-cold buffer containing: 50 mM Hepes (pH 7.6), 50 mM NaF, 50 mM KCl, 5 mM NaPPi, 1 mM EDTA, 1 mM EGTA, 1 mM DTT, 5 mM β-glycerophosphate, 1 mM sodium vanadate, 1% NP40 and protease inhibitors cocktail (Complete, Roche). Western blots were performed as previously described (35). Bands were visualized by enhanced chemiluminescence and quantified using Image J. Primary antibodies used are listed in Supplementary Table 3.

Statistical analysis

All data are presented as mean ± standard error of the mean (SEM). Statistical analysis was performed using GraphPad Prism 8.0 (GraphPad Software, La Jolla, CA, USA) with unpaired t-test, one-way or two-way analysis of variance (ANOVA) followed by Fisher's post-hoc test. Differences between groups were considered statistically significant at $P < 0.05$. Outliers were identified according to the two-standard deviation method.

Competing Interests statement

V. Chavanelle, Y. Otero, F. Le Joubioux, S.L. Peltier and P. Sirvent are all employees of Valbiotis. S.L. Peltier and P. Sirvent are listed as co-inventors on Totum-63 patent and possess company stock. None of the other authors have any potential conflict of interest. This work was supported in part by National Institute of Diabetes and Digestive and Kidney Diseases grants DK059637 and S10RR028101 (L.L., O. McG.), the NWO project 184.034.019 (M.G.), and Valbiotis (B.G.). Study design, collection of the data, analysis and interpretation of the results, writing and decision to submit the article for publication was performed by Guigas' group at the Leiden University Medical Center, in agreement with Valbiotis.

References

1. WHO. Obesity and overweight. Key facts.;https://www.who.int/news-room/fact-sheets/detail/obesity-and-overweight.
2. IDF. IDF Diabetes Atlas. 2019;9th edn:http://www.diabetesatlas.org/.
3. Williams R, Karuranga S, Malanda B, Saeedi P, Basit A, Besancon S, et al. Global and regional estimates and projections of diabetes-related health expenditure: Results from the International Diabetes Federation Diabetes Atlas, 9th edition. Diabetes Res Clin Pract. 2020;162:108072.
4. DeFronzo RA, Ferrannini E, Groop L, Henry RR, Herman WH, Holst JJ, et al. Type 2 diabetes mellitus. Nat Rev Dis Primers. 2015;1:15019.
5. Roden M, Shulman GI. The integrative biology of type 2 diabetes. Nature. 2019;576(7785):51-60.
6. Hotamisligil GS. Inflammation, metaflammation and immunometabolic disorders. Nature. 2017;542(7640):177-85.
7. Jais A, Bruning JC. Hypothalamic inflammation in obesity and metabolic disease. J Clin Invest. 2017;127(1):24-32.
8. Kazankov K, Jorgensen SMD, Thomsen KL, Moller HJ, Vilstrup H, George J, et al. The role of macrophages in nonalcoholic fatty liver disease and nonalcoholic steatohepatitis. Nat Rev Gastroenterol Hepatol. 2019;16(3):145-59.
9. Lackey DE, Olefsky JM. Regulation of metabolism by the innate immune system. Nat Rev Endocrinol. 2016;12(1):15-28.
10. Lee YS, Wollam J, Olefsky JM. An Integrated View of Immunometabolism. Cell. 2018;172(1-2):22-40.
11. Castejon-Vega B, Giampieri F, Alvarez-Suarez JM. Nutraceutical Compounds Targeting Inflammasomes in Human Diseases. Int J Mol Sci. 2020;21(14).
12. Granato D, Barba FJ, Bursac Kovacevic D, Lorenzo JM, Cruz AG, Putnik P. Functional Foods: Product Development, Technological Trends, Efficacy Testing, and Safety. Annu Rev Food Sci Technol. 2020;11:93-118.
13. Martel J, Ojcius DM, Chang CJ, Lin CS, Lu CC, Ko YF, et al. Anti-obesogenic and antidiabetic effects of plants and mushrooms. Nat Rev Endocrinol. 2017;13(3):149-60.
14. Alkhatib A, Tsang C, Tiss A, Bahorun T, Arefanian H, Barake R, et al. Functional Foods and Lifestyle Approaches for Diabetes Prevention and Management. Nutrients. 2017;9(12).
15. Kumar S, Pandey AK. Chemistry and biological activities of flavonoids: an overview. ScientificWorldJournal. 2013;2013:162750.
16. Hussain T, Tan B, Murtaza G, Liu G, Rahu N, Saleem Kalhoro M, et al. Flavonoids and type 2 diabetes: Evidence of efficacy in clinical and animal studies and delivery strategies to enhance their therapeutic efficacy. Pharmacol Res. 2020;152:104629.
17. Cory H, Passarelli S, Szeto J, Tamez M, Mattei J. The Role of Polyphenols in Human Health and Food Systems: A Mini-Review. Front Nutr. 2018;5:87.

18. Peltier S, Chavanelle V, Otero YF, Bargetto M, Cazaubiel M, Sirvent P, et al. Totum-63 Lowers Fasting Glycemia in Subjects with Prediabetes: A Phase 2A Clinical Trial. Diabetes. 2020;69(Supplement 1):848-P.
19. Inagaki T, Choi M, Moschetta A, Peng L, Cummins CL, McDonald JG, et al. Fibroblast growth factor 15 functions as an enterohepatic signal to regulate bile acid homeostasis. Cell Metab. 2005;2(4):217-25.
20. Tadera K, Minami Y, Takamatsu K, Matsuoka T. Inhibition of alpha-glucosidase and alpha-amylase by flavonoids. J Nutr Sci Vitaminol (Tokyo). 2006;52(2):149-53.
21. McDougall GJ, Kulkarni NN, Stewart D. Current developments on the inhibitory effects of berry polyphenols on digestive enzymes. Biofactors. 2008;34(1):73-80.
22. Tan Y, Chang SKC. Digestive enzyme inhibition activity of the phenolic substances in selected fruits, vegetables and tea as compared to black legumes. J Funct Foods. 2017;38:644-55.
23. Ko CW, Qu J, Black DD, Tso P. Regulation of intestinal lipid metabolism: current concepts and relevance to disease. Nat Rev Gastroenterol Hepatol. 2020;17(3):169-83.
24. Khoshbin K, Camilleri M. Effects of dietary components on intestinal permeability in health and disease. Am J Physiol Gastrointest Liver Physiol. 2020;319(5):G589-G608.
25. Patsouris D, Li PP, Thapar D, Chapman J, Olefsky JM, Neels JG. Ablation of CD11c-positive cells normalizes insulin sensitivity in obese insulin resistant animals. Cell Metab. 2008;8(4):301-9.
26. Han X, Zhang Y, Guo J, You Y, Zhan J, Huang W. Chlorogenic Acid Stimulates the Thermogenesis of Brown Adipocytes by Promoting the Uptake of Glucose and the Function of Mitochondria. J Food Sci. 2019;84(12):3815-24.
27. Oi-Kano Y, Kawada T, Watanabe T, Koyama F, Watanabe K, Senbongi R, et al. Oleuropein, a phenolic compound in extra virgin olive oil, increases uncoupling protein 1 content in brown adipose tissue and enhances noradrenaline and adrenaline secretions in rats. J Nutr Sci Vitaminol (Tokyo). 2008;54(5):363-70.
28. Ahmad TR, Haeusler RA. Bile acids in glucose metabolism and insulin signalling - mechanisms and research needs. Nat Rev Endocrinol. 2019;15(12):701-12.
29. Hussaarts L, Garcia-Tardon N, van Beek L, Heemskerk MM, Haeberlein S, van der Zon GC, et al. Chronic helminth infection and helminth-derived egg antigens promote adipose tissue M2 macrophages and improve insulin sensitivity in obese mice. FASEB J. 2015;29(7):3027-39.
30. van der Zande HJP, Gonzalez MA, de Ruiter K, Wilbers RHP, Garcia-Tardon N, van Huizen M, et al. The helminth glycoprotein omega-1 improves metabolic homeostasis in obese mice through type 2 immunity-independent inhibition of food intake. FASEB J. 2021;35(2):e21331.
31. Lantier L, Williams AS, Williams IM, Guerin A, Bracy DP, Goelzer M, et al. Reciprocity Between Skeletal Muscle AMPK Deletion and Insulin Action in Diet-Induced Obese Mice. Diabetes. 2020;69(8):1636-49.
32. Lee S, Muniyappa R, Yan X, Chen H, Yue LQ, Hong EG, et al. Comparison between surrogate indexes of insulin sensitivity and resistance and hyperinsulinemic euglycemic clamp estimates in mice. Am J Physiol Endocrinol Metab. 2008;294(2):E261-70.

33. Thomas A, Belaidi E, Aron-Wisnewsky J, van der Zon GC, Levy P, Clement K, et al. Hypoxia-inducible factor prolyl hydroxylase 1 (PHD1) deficiency promotes hepatic steatosis and liver-specific insulin resistance in mice. Sci Rep. 2016;6:24618.

34. Zinsou JF, Janse JJ, Honpkehedji YY, Dejon-Agobe JC, Garcia-Tardon N, Hoekstra PT, et al. Schistosoma haematobium infection is associated with lower serum cholesterol levels and improved lipid profile in overweight/obese individuals. PLoS Negl Trop Dis. 2020;14(7):e0008464.

35. Thomas A, Belaidi E, Moulin S, Horman S, van der Zon GC, Viollet B, et al. Chronic Intermittent Hypoxia Impairs Insulin Sensitivity but Improves Whole-Body Glucose Tolerance by Activating Skeletal Muscle AMPK. Diabetes. 2017;66(12):2942-51.

Supplementary Materials and Methods

Body composition and indirect calorimetry

Before the start of the measurements, the animals were acclimated to the cages and single housing for 48h. A standard 12h light/dark cycle was maintained throughout the calorimetry study. Spontaneous locomotor activity was determined by the measurement of beam breaks. Oxygen consumption and carbon dioxide production were measured at 30 sec intervals. Energy expenditure (EE) and carbohydrate (CHO) and fatty acid (FA) oxidation were calculated based on respirometry, as previously described (29). The ANCOVA analysis of EE was done using the NIDDK Mouse Metabolic Phenotyping Centers (www.mmpc.org).

Insulin- and glucose tolerance tests

For ipITT, a bolus of insulin (1U/kg lean body mass, Novorapid, Novo Nordisk) was administered i.p. in 4h-fasted mice after which blood glucose levels were measured at t=0, 20, 40, 60 and 90 min post insulin administration using a Glucometer (Accu-Check, Roche Diagnostics). For ipGTT, a bolus of glucose (2g D-Glucose/kg total body weight, Sigma-Aldrich) was administered i.p. in 6h-fasted mice and blood glucose was measured at t=0, 20, 40, 60 and 90 min post glucose injection.

Hyperinsulinemic-euglycemic clamp

Briefly, [3-^{3}H]-D-glucose was first primed and continuously infused (t=-90 to 0 min, 0.04 mCi/min). The insulin clamp was next initiated at t=0 min with a continuous insulin infusion (4 mU/kg/min) followed by variable glucose infusion rate (GIR) until t=155 min in order to maintain euglycemia. Arterial glucose levels were monitored every 10 min to provide feedback for adjustment of the GIR (50% dextrose + [3-^{3}H]-D-glucose). [3-^{3}H]-D-glucose kinetics were determined at t=-10 min and at steady state (from 80 to 120 min) to assess endogenous glucose production (EndoRa) and whole-body glucose disappearance (Rd) rates. An intravenous bolus of 2-[^{14}C]-deoxy-D-glucose (13 μCi) was administered at t=120 min. The mice were sacrificed at t=155 min and their tissues immediately harvested and freeze-clamped to determine glucose metabolic index (Rg), an index of tissue-specific glucose uptake. Plasma and tissue processing were performed as previously described (31). Full step-by-step descriptions of the HI-EU clamp and calculations are available from the Vanderbilt Mouse Metabolic Phenotyping Center website (www.vmmpc.org).

Hepatic lipid composition

Liver TG and TC concentrations were measured using the commercial kits described above and expressed as mg per mg of total protein content using the Bradford protein assay kit (Sigma-Aldrich). For lipidomics, lipids were extracted from 10 mg of liver by the methyl-tert-butylether method and analyzed using the Lipidyzer™, a direct infusion-tandem mass spectrometry (DI-MS/MS)-based platform (Sciex, Redwood City, USA), as previously described (34). Lipid concentrations were expressed as pmol/mg of liver.

Feces lipid composition

Lipids were extracted from 50 mg of collected 24h after cage refreshment by the same method described above for the liver and analyzed using the Lipidyzer™ platform. Lipid concentrations were expressed as pmol/mg of fresh feces.

Isolation of stromal vascular fraction from adipose tissue

eWAT samples were minced and incubated for 1 hour at 37°C in an incubator under agitation (60 rpm) containing 0.5 g/L collagenase type I from *Clostridium histolyticum* (Sigma-Aldrich), 100 mM HEPES (ThermoFisher), 2% (w/v) dialyzed bovine serum albumin (BSA, fraction V; Sigma-Aldrich) and 6 mM D-Glucose. The samples were passed through a 236 µm filter which was washed with PBS supplemented with 2.5 mM EDTA and 1% FCS. Adipocytes and stromal vascular fraction (SVF) were separated by collecting the infranatant. SVF was next pelleted at 350 x g for 10 min at room temperature and treated with erythrocyte lysis buffer (0.15 M NH_4Cl; 1 mM $KHCO_3$; 0.1 mM Na_2EDTA). Cells were washed with PBS/EDTA/FCS, and counted using a hematocytometer, as previously described (29, 30).

Isolation of liver leukocytes

Livers were minced and incubated for 45 min at 37°C in RPMI 1640 + Glutamax (Life Technologies) containing 1 mg/ml collagenase type IV from *Clostridium histolyticum*, 200 U/ml DNase (both Sigma-Aldrich) and 1 mM $CaCl_2$. The digested tissues were passed through a 100 µm cell strainer which was subsequently washed with PBS/EDTA/FCS. After washing the pellet once with PBS/EDTA/FCS, the samples were centrifuged at 50 x g for 3 minutes at 4°C to pellet the hepatocytes. The supernatant was collected and spun down at 530 x g for 10 min at 4°C. The pellet was subsequently treated with erythrocyte lysis buffer and next washed with PBS/EDTA/FCS. $CD45^+$ leukocytes were isolated using LS columns and CD45 MicroBeads (35 µL beads per sample, Miltenyi Biotec) according to the manufacturer's protocol and the isolated cells were counted using a hematocytometer, as described previously (29, 30).

Isolation of blood leukocytes

Blood was treated with erythrocyte lysis buffer. After washing, cells were centrifuged (530 x g, 10 min at 4°C), resuspended in FACS buffer, counted, and processed as described above for the SVF from eWAT.

Flow cytometry

For analysis of WAT and liver myeloid subsets, cells were first permeabilized with 0.5% saponin (Sigma-Aldrich) and stained with an antibody against YM1 conjugated to biotin. After washing, cells were next stained with streptavidin-PerCP (BD Biosciences) and antibodies directed against CD45.2, Siglec-F, CD11b, Ly6C, F4/80 and CD11c in 0.5% saponin/FACS buffer. For analysis of blood monocyte and lymphocyte subsets, cells were first permeabilized or not with 0.5% saponin (Sigma-Aldrich), respectively. After washing, cells were stained with antibodies directed against CD45.2, Siglec-F, CD11b, Ly6C, B220 and CCR2 (monocyte subset) or CD45.2, CD19, NK1.1, CD3, CD4 and CD8 (lymphocyte subset). Cells were measured on a FACSCanto or LSR-II flow cytometer (BD Biosciences), and gates were set according to Fluorescence Minus One (FMO) controls. Antibody information is provided in Supplementary Table 4.

Supplementary references

1. L. Hussaarts, N. Garcia-Tardon, L. van Beek, M.M. Heemskerk, S. Haeberlein, G.C. van der Zon, A. Ozir-Fazalalikhan, J.F. Berbee, K. Willems van Dijk, V. van Harmelen, M. Yazdanbakhsh, and B. Guigas, Chronic helminth infection and helminth-derived egg antigens promote adipose tissue M2 macrophages and improve insulin sensitivity in obese mice. FASEB J 29 (2015) 3027-39.
2. L. Lantier, A.S. Williams, I.M. Williams, A. Guerin, D.P. Bracy, M. Goelzer, M. Foretz, B. Viollet, C.C. Hughey, and D.H. Wasserman, Reciprocity Between Skeletal Muscle AMPK Deletion and Insulin Action in Diet-Induced Obese Mice. Diabetes 69 (2020) 1636-1649.
3. J.F. Zinsou, J.J. Janse, Y.Y. Honpkehedji, J.C. Dejon-Agobe, N. Garcia-Tardon, P.T. Hoekstra, M. Massinga-Loembe, P. Corstjens, G.J. van Dam, M. Giera, P.G. Kremsner, M. Yazdanbakhsh, A.A. Adegnika, and B. Guigas, Schistosoma haematobium infection is associated with lower serum cholesterol levels and improved lipid profile in overweight/obese individuals. PLoS Negl Trop Dis 14 (2020) e0008464.
4. H.J.P. van der Zande, M.A. Gonzalez, K. de Ruiter, R.H.P. Wilbers, N. Garcia-Tardon, M. van Huizen, K. van Noort, L.R. Pelgrom, J.M. Lambooij, A. Zawistowska-Deniziak, F. Otto, A. Ozir-Fazalalikhan, D. van Willigen, M. Welling, J. Poles, F. van Leeuwen, C.H. Hokke, A. Schots, M. Yazdanbakhsh, P. Loke, and B. Guigas, The helminth glycoprotein omega-1 improves metabolic homeostasis in obese mice through type 2 immunity-independent inhibition of food intake. FASEB J 35 (2021) e21331.

Supplementary information

Supplementary Table 1. Chemical characterization of Totum-63.

Compound type	Extract content (g/100 g dry weight)
Total polyphenols	14.36
Total anthocyanins	0.81
Monocaffeoylquinic acids	1.18
Chlorogenic acid	0.85
Other monocaffeoylquinic acids	0.33
Dicaffeoylquinic acids	0.98
Cynarin	0.24
Other dicaffeoylquinic acids	0.74
Caffeic acid	0.01
Oleuropein	3.72
Oleuropein isomers	0.20
Hydroxytyrosol	0.04
Luteolin	0.01
Luteolin-7-O-glucoside	0.38
Luteolin-7-O-glucuronide	0.38
Apigenin	0.01
Apigenin-7-O-glucoside	0.01
Apigenin-7-O-glucuronide	0.25
Apigenin 6-C-glucoside-8-C-arabinoside (Shaftoside)	0.06
Apigenin 6,8-C-diglucoside (Vicenin 2)	0.06
Eriodictyol	<0.01
Eriodictyol-7-O-glucoside	0.11
Okanin-4-O-glucoside (Marein)	0.05
Isookanin-7-O-glucoside (Flavanomarein)	0.05
Maritimetin-6-O-glucoside (Maritimein)	0.08
Saponins	
Chrysanthellin A	0.01
Chrysanthellin B	0.27
Alkaloid	
Piperin	0.004
Fiber	
Soluble Fiber	13.7
Insoluble Fiber	3.3

Supplementary Table 2. qPCR primers.

Gene	Accession number	Forward primer	Reverse primer
Abcg5	NM_031884	TGTCCTACAGCGTCAGCAACC	GGCCACTCTCGATGTACAAGG
Abcg8	NM_026180	TCCTGTGAGCTGGGCATCCGA	CCCGCAGCCTGAGCTCCCTAT
Acaca	NM_133360.2	CAGCTGGTGCAGAGGTACCG	TCTACTCCGCAGGTACTGCCG
Acox1	NM_015729	GGGACCCACAAGCCTCTGCCA	GTGCCGTCAGGCTTCACCTGG
Acta2	NM_007392.3	AGCCATCTTTCATTGGGATGG	CCCCTGACAGGACGTTGTTA
Adgr1	NM_010130.4	CTTTGGCTATGGGCTTCCAGTC	GCAAGGAGGACAGAGTTTATCGTG
Adrb3	NM_013462.3	CACCGCTCAACAGGTTTGATG	TCTTGGGGCAACCAGTCAAG
Cck	NM_031161.4	CTGCCCTCAACTTAGCTGGA	TTCATGGCTTTGGATGGGGAA
Ccl2	NM_011333.3	TCAGCCAGATGCAGTTAACGCCC	GCTTCTTTGGGACACCTGCTGCT
Cd3e	NM_007648.4	CAGGACGATGCCGAGAACATT	CGTCACTGTCTAGAGGGCAC
Cd36	NM_001159558	GCAAAGAACAGCAGCAAAATC	CAGTGAAGGCTCAAAGATGG
Cd68	NM_009853.1	CCTCCACCCTCGCCTAGTC	TTGGGTATAGGATTCGGATTTGA
Cdh1	NM_009864.3	CCAAGCACGTATCAGGGTCA	ACTGCTGGTCAGGATCGTTG
Cidea	NM_007702	CTCGGCTGTCTCAATGTCAA	CCGCATAGACCAGGAACTGT
Cidec	NM_178373	CCATCAGAACAGCGCAAGAAG	AGAGGGTTGCCTTCACGTTC
Cldn3	NM_009902.4	CCTAGGAACTGTCCAAGCCG	CCCGTTTCATGGTTTGCCTG
Clec4f	NM_016751.3	ACTGAAGTACCAAATGGACAATGTTAGT	GTCAGCATTCACATCCTCCAGA
Col1a1	NM_007742.3	GAGAGGTGAACAAGGTCCCG	AAACCTCTCTCGCCTCTTGC
Cox8b	NM_007751.3	GACCCCGAGAATCATGCCAA	CCTGCTCCACGGCGGAA
Cpt1a	NM_013495	AGGAGACAAGAACCCCAACA	AAGGAATGCAGGTCCACATC
Dgat2	NM_026384.3	GTCTCCTGGCTAGGGACACG	GGATATGCGCCAGAGCAACG
Dio2	NM_010050	CGCTCCAAGTCCACTCGCGG	CGGCCCCATCAGCGGTCTTC
Fabp1	NM_017399.4	GCCACCATGAACTTCTCCGGCA	GGTCCTCGGGCAGACCTATTGC
Fas	NM_007988	CACAGGCATCAATGTCAACC	TTTGGGAAGTCCTCAGCAAC
Fbp1	NM_019395.2	GCATCGCACAGCTCTATGGT	ACAGGTAGCGTAGGACGACT
Fgf15	NM_008003.2	CGGTCGCTCTGAAGACGATT	CCTCCGAGTAGCGAATCAGC
G6pc	NM_008061	CCATGGGCGCAGCAGGTGTA	AGCCACGACCTGGTGGGGAA
Gcg	NM_008100.4	TTGAGAGGCATGCTGAAGGG	TCTTCTGGGAAGTCTCGCCT

Gene	Accession number	Forward primer	Reverse primer
Gdf15	NM_011819.3	GTCCAGAGGTGAGATTGGGG	CTTCAGGGGCCTAGTGATGTC
Ghrl	NM_021488.5	CCAGAAAGCCCAGCAGAGAAAG	ATGCCAACATCGAAGGGAGC
Hhip	NM_020259.4	ATACCACCAACCAGGAACGG	GGGGGTTTTTCCTGGATACTGT
Infg	NM_008337	CGGCACAGTCATTGAAAGCC	TGTCACCATCCTTTTGCCAGT
Il1b	NM_008361	GACCCCAAAAGATGAAGGGCT	ATGTGCTGCTGCGAGATTTG
Il10	NM_010548	GACAACATACTGCTAACCGACTC	ATCACTCTTCACCTGCTCCACT
Itgax	NM_021334.2	GCCACCAACCCTTCCTGGCTG	TTGGACACTCCTGCTGTGCAGTTG
Lcn2	NM_008491	GCCACTCCATCTTTCCTGTTG	AAGAGGCTCCAGATGCTCCTT
Lep	NM_008493	CCCTGTGTCGGTTCCTGTGGC	GCGGATACCGACTGCGTGTGT
Ncub2	NM_001360375.1	GTATCATCAGGCCGTCCAGC	CAAACTTCAGCTCTCCCGCT
Ocln	NM_001360536.1	GTCCTCCTGGCTCAGTTGAA	AGATAAGCGAACCTTGGCGG
Pck1	NM_011044.2	GGGCCGCTGGATGTCGGAAG	GGTGCGGCCTTTCATGCACC
Ppara	NM_011144	CAACCCGCCTTTTGTCATAC	CCTCTGCCTCTTTGTCTTCG
Ppargc1a	NM_008904.2	CCCAGAGTCACCAAATGACCCCA	CCTCTTGGTTGGCGGTGGCA
Pyy	NM_145435.1	GGCAGCGGTATGGAAAAAGA	CCACTGGTCCAAACCTTCTG
Rplp0	NM_007475	TCTGGAGGGTGTCCGCAACG	GCCAGGACGCGCTTGTACCC
Scd1	NM_009127.4	GCTCTACACCTGCCTCTTCGGGAT	TCCAGAGGCGATGAGCCCCG
Slc2a2	NM_031197.2	TCATGTCGGTGGGACTTGTG	CCCAAGGAAGTCCGCAATGT
Slc5a1	NM_019810.4	AGTGGGCTGTACCAACATCG	CAGGCCTCGCAGTCCATTAG
Srebp1	NM_011480	CTGGCTGAGGCGGGATGA	TACGGGCCACAAGAAGTAGA
Tbx1	NM_011532.2	CAAGGCAGGCAGACGAATGT	TACCGGTAGCGCTTGTCATC
Timp1	NM_011593	AGTGCCTGCAGCTTCTTGGT	CAGCCAGCACTATAGGTCTTTGAG
Tjp1	NM_009386.2	GGAGATGTTTATGCGGACGG	CCATTGCTGTGCTCTTAGCG
Tnfa	NM_013693	GTCCCCAAAGGGATGAGAAG	CACTTGGTGGTTTGCTACGA
Ucp1	NM_009463	TCAGGATTGGCCTCTACGAC	TGCATTCTGACCTTCACGAC

Supplementary Table 3. Western Blot antibodies.

Primary antibody	Residue	Supplier	Reference	Dilution
HSP90	-	Santa Cruz	sc-7947	1:1000
IRβ	-	Santa Cruz	sc-711	1:1000
PKBα	-	Upstate	07-416	1:1000
PKBβ	-	Upstate	07-372	1:1000
Phospho-PKB	Ser473	Cell Signaling	#9271	1:1000
UCP1	-	Abcam	ab10983	1:1000

Supplementary Table 4. FACS antibodies.

Target	Clone	Conjugate	Source	Identifier
B220	RA3-6B2	FITC	eBioscience	11-0452
B220	RA3-6B2	eF450	eBioscience	48-0452
CCR2	475301	APC	R&D Systems	FAB5538A
CD3e	17A2	APC	eBioscience	17-0032
CD4	GK1.5	PE-Cy7	eBioscience	25-0041
CD8a	53-6.7	APC-Cy7	Biolegend	100714
CD11b	M1/70	PE-Cy7	eBioscience	25-0112
CD11c	N418	BV421	Biolegend	117330
CD19	eBio1D3	eF450	eBioscience	48-0193
CD45	30-F11	BV785	Biolegend	103149
CD45.2	104	FITC	Biolegend	109806
F4/80	BM8	APC	eBioscience	17-4801
Ly6C	HK1.4	APC-Cy7	Biolegend	128025
NK1.1	PK136	PE	BD Biosciences	557391
Siglec-F	E50-2440	BV605	BD Biosciences	740388
Siglec-F	E50-2440	PE	BD Biosciences	552126
Other reagents			**Source**	**Identifier**
LIVE/DEAD™ Fixable Aqua Dead Cell Stain Kit			Invitrogen	L34957
Zombie UV™ Fixable Viability Kit			Biolegend	423107

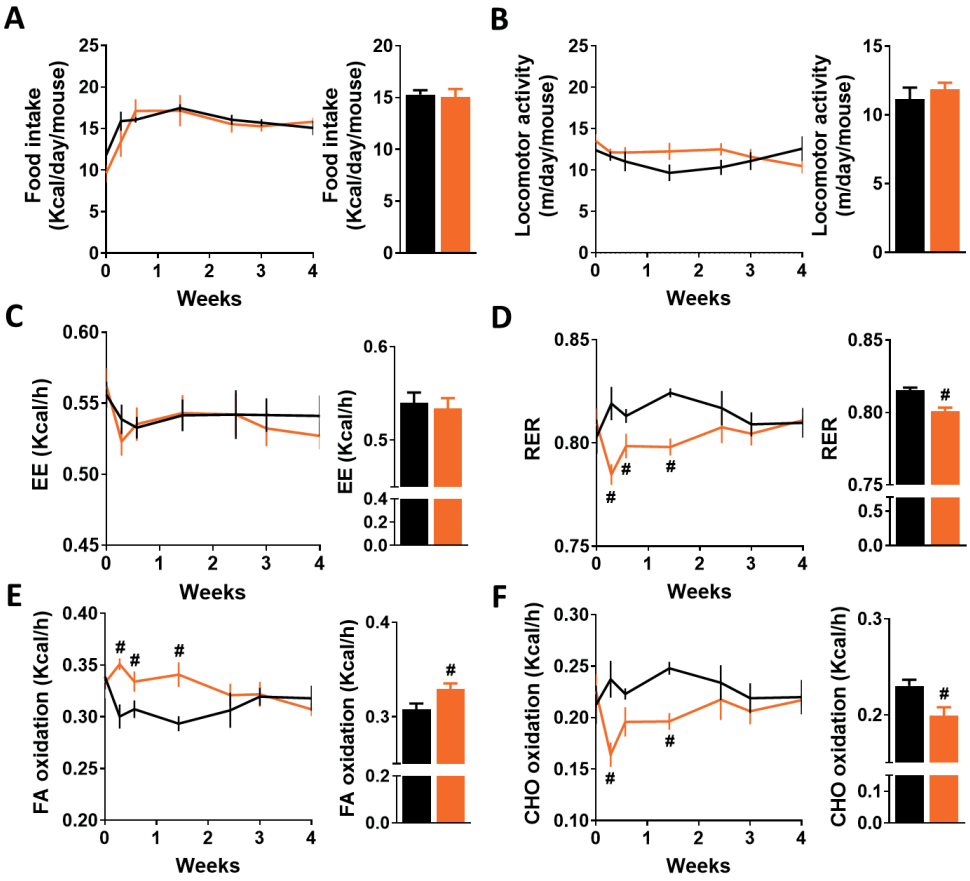

Supplementary Figure 1. Totum-63 does not affect food intake, locomotor activity and total energy expenditure, but promotes a shift towards fatty acid oxidation in obese mice. C57BL6/J mice were fed a HFD for 12 weeks and next transferred to individual metabolic cages. After 48 hours of acclimatization, mice received HFD supplemented or not with Totum-63 (2.7% w/w) for 4 weeks. (**A-B**) Food intake (*A*) and locomotor activity (*B*) were monitored throughout the study. (**C-F**) Oxygen consumption and carbon dioxide production were measured at 30 sec intervals and total energy expenditure (EE, *C*), respiratory exchange ratio (RER, *D*), and fatty acid (FA, *E*) and carbohydrate (CHO, *F*) oxidation rates were calculated, and the averaged data during 4 weeks were shown. Results are expressed as mean ± SEM. # P ≤ 0.05 *vs* HFD (n=8 mice per group from 2 independent experiments).

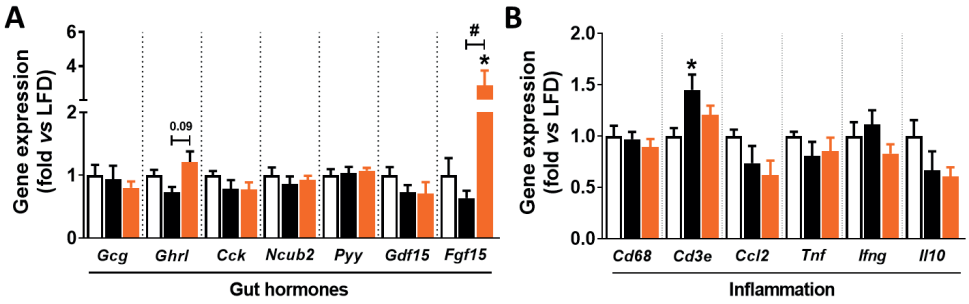

Supplementary Figure 2. Totum-63 does not affect the gene expression of main gut hormones and inflammatory markers in ileum from obese mice. LFD- and HFD-fed C57BL6/J mice were treated as described in the legend of Figure 1. (**A-B**) The expression of key genes involved in gut hormone synthesis (*A*) and inflammation (*B*) was measured in the ileum section of the intestine by RT-qPCR. Results are expressed as mean ± SEM. * P ≤ 0.05 *vs* LFD, # P ≤ 0.05 *vs* HFD (n=5-6 mice per group).

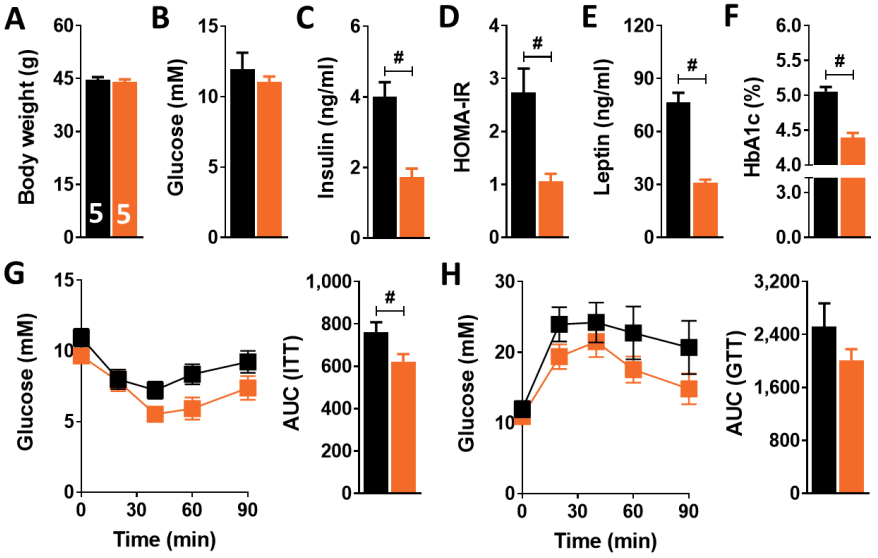

Supplementary Figure 3. Totum-63 improves metabolic homeostasis in obese mice independently of its effect on body weight. (**A**) C57BL6/J obese mice on HFD supplemented with Totum-63 (T63, 2.7% w/w; orange squares/bars) or not (control; black squares/bars) were weight-paired after 4 weeks of supplementation. (**B-F**) Fasting blood glucose (*B*) and HbA1c (*F*) levels together with plasma insulin (*C*) and leptin (*E*) levels, and HOMA-IR (*D*) were determined. (**G-H**) Intraperitoneal ITT (*G*) and GTT (*H*) were performed and the respective AUC calculated, as described in the legend of Figure 3. Results are expressed as mean ± SEM. * P ≤ 0.05 *vs* LFD, # P ≤ 0.05 *vs* HFD (n=5 mice selected per group from 2 independent experiments).

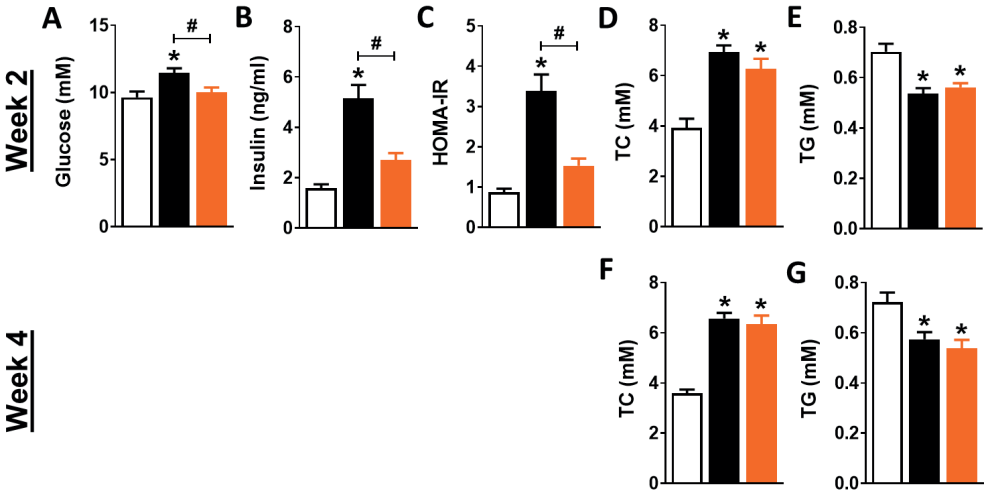

Supplementary Figure 4. Totum-63 reduces hyperglycemia and hyperinsulinemia already after 2 weeks but does not affect plasma TC and TG levels in obese mice. LFD- and HFD-fed C57BL6/J mice were treated as described in the legend of Figure 1. (**A-C**) Fasting blood glucose (*A*) and plasma insulin (*B*) levels were measured at week 2 of supplementation and used to calculate the HOMA-IR (*C*). (**D-G**) Fasting plasma total cholesterol (TC, *D,F*) and triglycerides (TG, *E,G*) were also determined at week 2 (*D-E*) and 4 (*F-G*). Results are expressed as mean ± SEM. * P ≤ 0.05 *vs* LFD, # P ≤ 0.05 *vs* HFD (n=10-12 mice per group from 2 independent experiments).

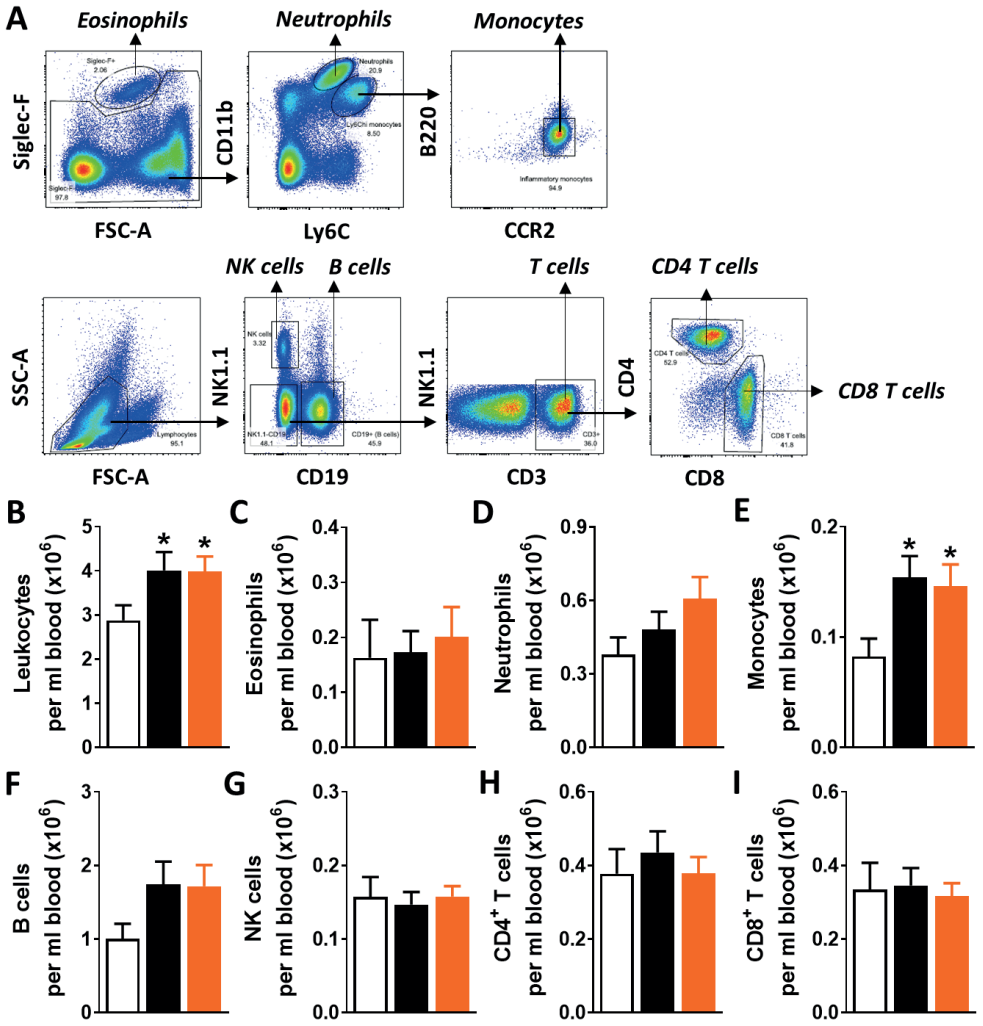

Supplementary Figure 5. Totum-63 does not affect blood immune cell subsets in obese mice. LFD- and HFD-fed C57BL6/J mice were treated as described in the legend of Figure 1. (**A**) The gating strategy for analysis of blood eosinophils, neutrophils, monocytes, NK cells, B cells, and CD4/CD8 T cells is shown for a representative sample. Isolated cells were pre-gated on $CD45^+$ single cells. (**B-I**) The blood levels of $CD45^+$ leukocytes (*B*), monocytes (*C*), neutrophils (*D*), eosinophils (*E*), B cells (*F*), NK cells (*G*), CD4 T cells (*H*) and CD8 T cells (*I*) were determined by flow cytometry. Results are expressed as mean ± SEM. * $P \leq 0.05$ *vs* LFD, # $P \leq 0.05$ *vs* HFD (n=4-6 mice per group).

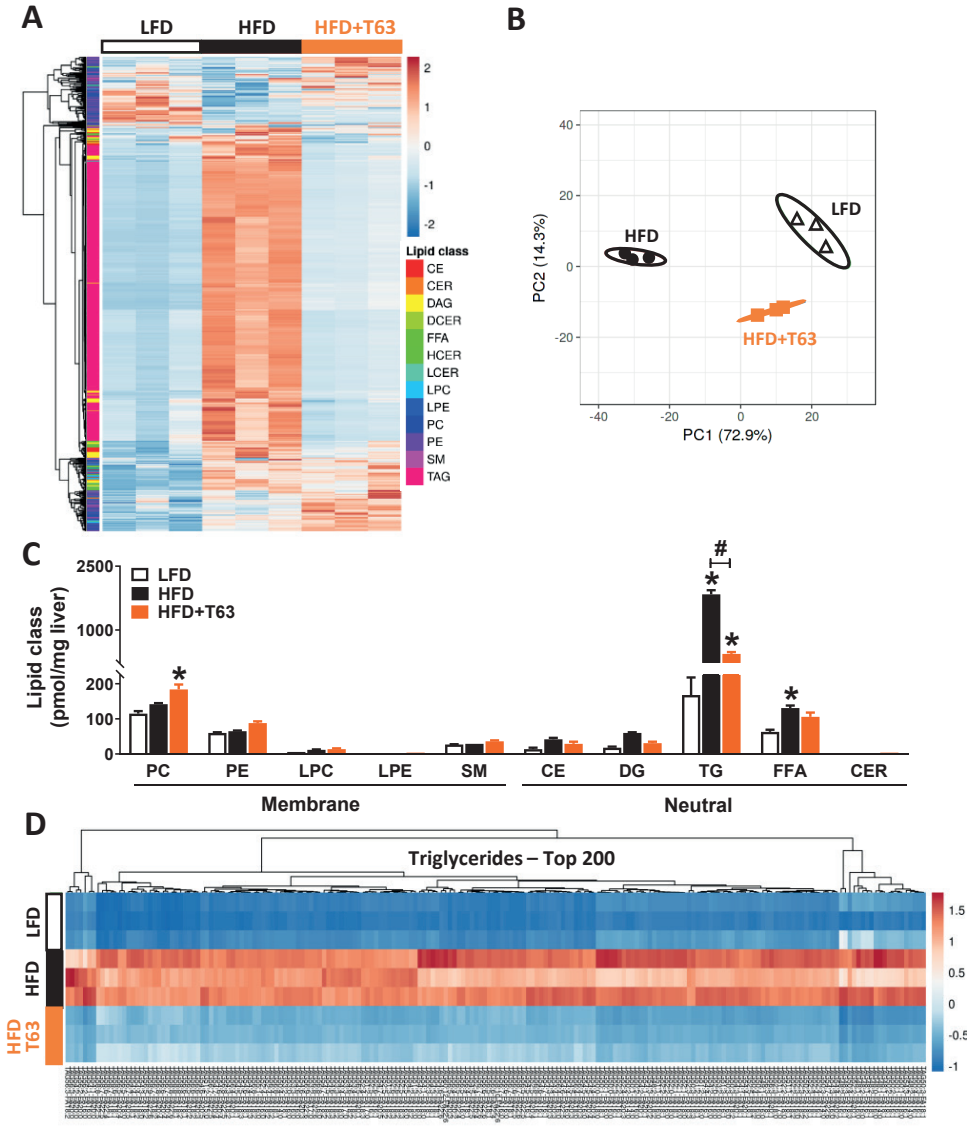

Supplementary Figure 6. Totum-63 reduces accumulation of hepatic triglyceride species in obese mice. LFD- and HFD-fed C57BL6/J mice were treated as described in the legend of Figure 1. (**A-D**) At sacrifice, a piece of liver was collected and freeze-clamped. After lipid extraction, the hepatic lipid species concentrations were quantified by targeted lipidomics using the Lipidyzer platform. The heatmap (*A*) and PCA plot (*B*) depicting the effect of T63 on >800 individual lipid species are shown. The levels of the individual lipid species were summed up for each lipid class (*C*) and the heatmap for the top 200 triglyceride species expressed is shown (*D*). PC, Phosphatidylcholine; PE, Phosphatidylethanolamine; LPC, Lysophosphatidylcholine; LPE, Lysophosphatidylethanolamine; SM, Sphingomyelin; CE, Cholesterylester; DG, Diglycerides; TG, Triglycerides; FFA, Free-fatty acids; CER, Ceramides. Results are expressed as mean ± SEM. * P ≤ 0.05 *vs* LFD, # P ≤ 0.05 *vs* HFD (n=3 mice per group).

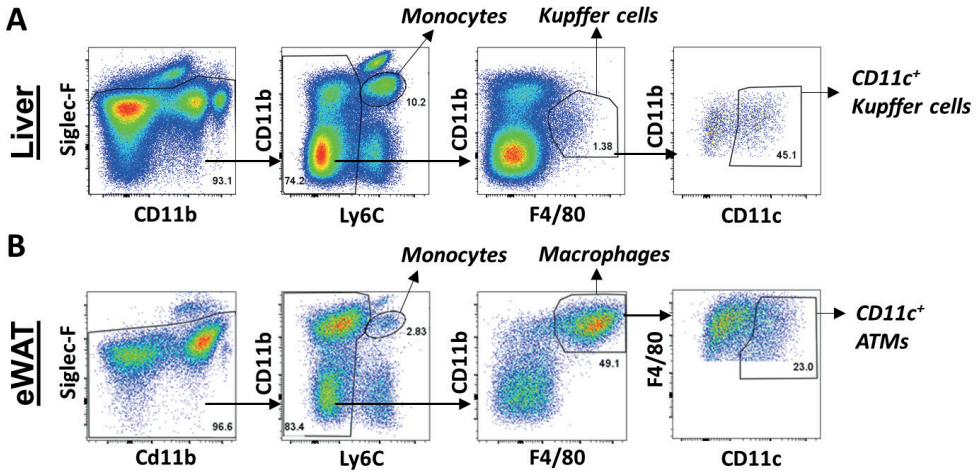

Supplementary Figure 7. Gating strategies for liver and adipose tissue immune cell phenotyping. (**A-B**) Isolated cells from liver (*A*) or eWAT (*B*) were pre-gated on Aqua^{-}CD45^{+} single cells. The gating strategy for analysis of monocytes, Kupffer cells (KC)/adipose tissue macrophages (ATMs) and CD11c^{+} KC/ATMs is shown for a representative sample.

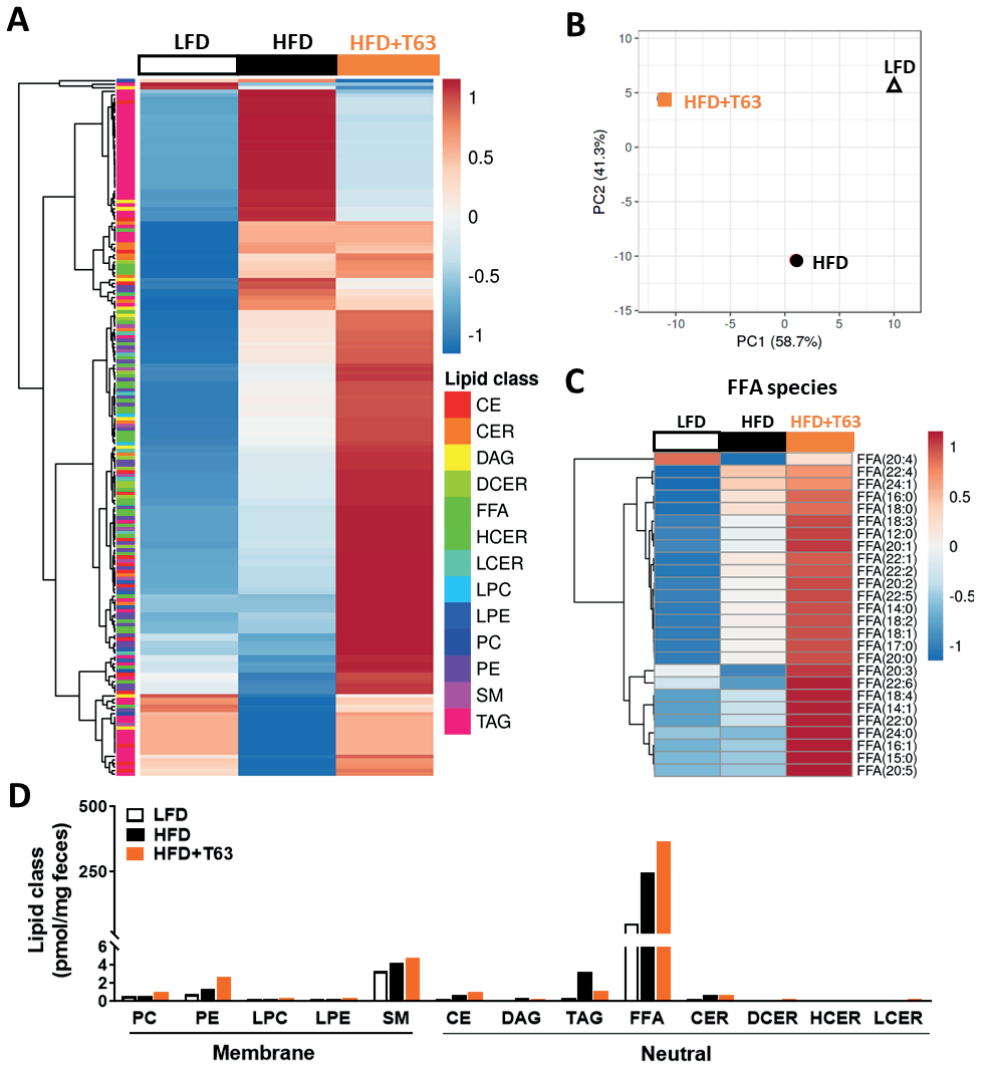

Supplementary Figure 8. Feces lipid composition from obese mice is affected by Totum-63. LFD- and HFD-fed C57BL6/J mice were treated as described in the legend of Figure 1. (**A-D**) Overnight-produced feces were collected and freeze-clamped. After lipid extraction, the feces lipid species concentrations were quantified by targeted lipidomics using the Lipidyzer platform. The heatmap (*A*) and PCA plot (*B*) depicting the effect of T63 on >800 individual lipid species are shown. The heatmap for the free fatty acid species expressed is shown (*C*) and the individual lipid species were summed up for each lipid class (*D*). PC, Phosphatidylcholine; PE, Phosphatidylethanolamine; LPC, Lysophosphatidylcholine; LPE, Lysophosphatidylethanolamine; SM, Sphingomyelin; CE, Cholesterylester; DG, Diglycerides; TG, Triglycerides; FFA, Free-fatty acids; CER, Ceramides. Results are data from pooled feces per group (n=3-4 cages per group).